Caged Biomolecules

International Edition: DOI: 10.1002/anie.201603281
German Edition: DOI: 10.1002/ange.201603281

Three-Dimensional Control of DNA Hybridization by Orthogonal Two-Color Two-Photon Uncaging

*Manuela A. H. Fichte, Xenia M. M. Weyel, Stephan Junek, Florian Schäfer, Cyril Herbivo, Maurice Goeldner, Alexandre Specht, Josef Wachtveitl, and Alexander Heckel**

Abstract: *We successfully introduced two-photon-sensitive photolabile groups ([7-(diethylamino)coumarin-4-yl]methyl and p-dialkylaminonitrobiphenyl) into DNA strands and demonstrated their suitability for three-dimensional photorelease. To visualize the uncaging, we used a fluorescence readout based on double-strand displacement in a hydrogel and in neurons. Orthogonal two-photon uncaging of the two cages is possible, thus enabling complex scenarios of three-dimensional control of hybridization with light.*

The control of biological systems dose-dependently in time and space is a key prerequisite for studying dynamic cellular processes in tissues or organisms in vivo. An ideal trigger signal for this purpose is light.[1–5] "Caged compounds" have photolabile groups installed in key places to temporarily render biologically active compounds inactive.[6–9] This approach typically leads to excellent ON/OFF behavior and has formed the basis of very interesting studies in chemical biology and material sciences[10–12] and enabled the construction of useful nanoarchitectures,[13] such as caged nanovehicles for drug release.[14]

Ideally, the release wavelength is in a part of the spectrum which is far away from the UV-C and UV-B regions to avoid unwanted side reactions and as far redshifted as possible for best tissue penetration, thus avoiding the absorbance by hemoglobin ($\lambda > 600$ nm).[15,16] The ultimate goal would be three-dimensional resolution, despite the fact that the controlling light passes as a straight beam through the medium. Two-photon excitation can achieve all these goals.[17] For example, tissue penetration of near-IR light reaches up to 1 cm.[16] In this nonlinear optical technique, the carbon–heteroatom bond is cleaved by irradiation at roughly half the normally required energy. In contrast to normal one-photon excitation, the efficiency of this effect depends on the square of the photon flux density. With suitable optical parameters of high numerical aperture and long working distance, it is possible to achieve a photochemical reaction volume of ellipsoidal shape as small as 1 fL with pulsed femtosecond lasers (see Figure S1 in the Supporting Information for an illustration).[18]

The development of new two-photon-sensitive caging groups is very difficult, especially if they are to be applied in an aqueous context. Seminal contributions include, for example, coumarin,[19–22] quinoline,[23,24] nitroindole,[25] hydroxycinnamate,[26] pyridinium,[27] nitrobenzyl,[28–31] and nitrophenethyl[30] derivatives. Examples of interesting applications of two-photon uncaging include caged neurotransmitters or Ca^{2+}[19,28,30,32] and the local structuring of gels and surfaces.[10–12,33] Two-photon uncaging of peptides has also been studied.[34–37]

In the field of the light regulation of nucleic acids we know of only one type of study (besides others on caged nucleoside monomers[38,39]), in which NIR-to-UV upconversion nanoparticles were used for the release of siRNA, albeit with lower efficiency and without 3D resolution.[40,41] Also, Chen and coworkers demonstrated the two-photon activation of morpholino oligonucleotides by using photolabile linkers.[42]

The aim of the present study was to directly introduce two-photon-sensitive caged phosphoramidites into DNA and prove that hybridization could be controlled with 3D resolution. By optimizing the design, we even developed "orthogonal" two-color two-photon uncaging. This term was originally coined by Bochet[43] and refers to a set of coexisting photolabile groups that can each be addressed selectively while leaving the others untouched. This characteristic allows for much more sophisticated scenarios of light regulation and has been reported previously by Ellis-Davies and co-workers for caged neurotransmitters in the two-photon domain.[20,44]

As the two uncaging chromophores for this study, we chose [7-(diethylamino)coumarin-4-yl]methyl (DEACM) and *p*-dialkylaminonitrobiphenyl (ANBP), for which two-photon action cross-sections of 0.12[22] and 11 GM,[33] respectively, were determined previously at 800 nm (Figure 1). The first was used to nucleobase-protect a dT residue,[45] whereas the latter was installed on a dG residue (see the Supporting Information for synthetic details). Both residues were introduced via their protected phosphoramidites into two separate

[*] M. A. H. Fichte, X. M. M. Weyel, Dr. F. Schäfer, Prof. Dr. A. Heckel
Institute of Organic Chemistry and Chemical Biology
Goethe-University Frankfurt
Max-von-Laue-Strasse 9, 60438 Frankfurt am Main (Germany)
E-mail: heckel@uni-frankfurt.de
Prof. Dr. J. Wachtveitl
Institute of Physical and Theoretical Chemistry
Goethe University Frankfurt
Max-von-Laue-Strasse 7, 60438 Frankfurt am Main (Germany)
Dr. S. Junek
Imaging Facility, Max Planck Institute for Brain Research
Max-von-Laue-Strasse 4, 60438 Frankfurt am Main (Germany)
Dr. C. Herbivo, Prof. Dr. M. Goeldner, Dr. A. Specht
Centre National de la Recherche Scientifique
Université de Strasbourg, Unité Mixte de Recherche 7199
Laboratoire de Conception et Application de Molécules Bioactives
Équipe de Chimie et Neurobiologie Moléculaire
67400 Illkirch (France)
Supporting information and the ORCID identification number(s) for the author(s) of this article can be found under http://dx.doi.org/10.1002/anie.201603281.

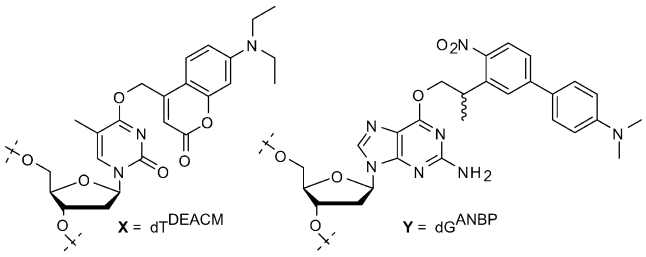

Figure 1. Two different caged thiol-modified DNA sequences were used in this study: **DNA 1** and **DNA 2**. X and Y represent the caged nucleotides dT^{DEACM} and dG^{ANBP}. The thiol modification is introduced for the immobilization of the DNA strands in a maleimide-modified hydrogel.

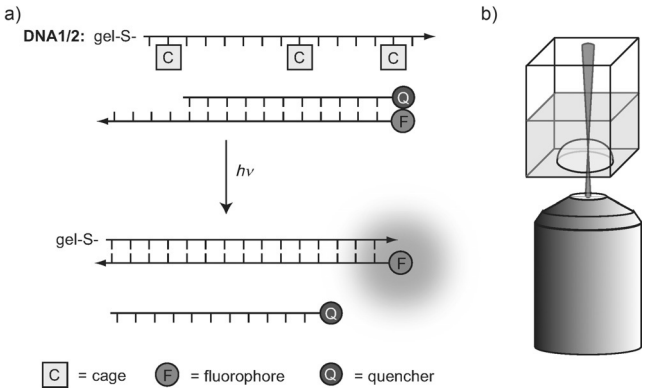

Figure 2. Schematic representation of a) the strand-displacement strategy used for the visualization of one-photon and two-photon uncaging and b) the irradiation setup. For further details, see the main text.

DNA sequences by solid-phase synthesis. Additionally, the strands were modified with a thiol functionality at the 5′-end for immobilization purposes.

One main challenge is the visualization and quantification of the two-photon uncaging process and the proof of non-linear excitation. In the case of the two-photon release of neurotransmitters or of Ca^{2+}, the process can be observed and quantified indirectly on the basis of biological effects.[19,28,30,32]

Unfortunately, the uncaging of **DNA 1** and **DNA 2** cannot be followed directly by spectroscopic techniques. Whereas the removal of caging groups leads to dramatic changes observable by RP-HPLC,[45] two-photon uncaging is meant to only involve the irradiation of a minimal part of the sample. More problematically, the femtosecond lasers used operate at an 80 MHz repetition rate. It is not practical to move the sample or the beam fast enough to prevent irradiation of already uncaged sample regions. The kinetics are then dominated by the diffusion time of new, caged compounds into the two-photon focus. Also, extensive two-photon irradiation generates undesired amounts of heat in the sample. Indeed, our results obtained with this method were difficult to interpret quantitatively.

Therefore, we decided to set up a fluorescence-based assay.[46] To this end, we used a strand-displacement assay in which **DNA 1** or **DNA 2** was immobilized in a maleimide-functionalized polyvinyl alcohol hydrogel. For each of the two strands we designed a DNA duplex probe which consisted of a corresponding antisense strand that was 5′-labeled with a fluorophore and a shorter sense strand that was 3′-labeled with a quencher (Figure 2; see also the Supporting Information). ATTO565 and BHQ2 were used as the fluorophore/quencher pair in the probe for **DNA 1**, and ATTO Rho14 and BBQ650 were used in the probe for **DNA 2**. Only upon uncaging is the shorter sense strand displaced, thus marking the uncaging site with the characteristic emission of the respective fluorophore.

Figure 3 shows the results obtained when a hydrogel containing **DNA 1** and the corresponding probe were irradiated at 780 nm in a microscope equipped with a suitable laser for two-photon excitation and a scanning head (see the Supporting Information for details). For each of the data

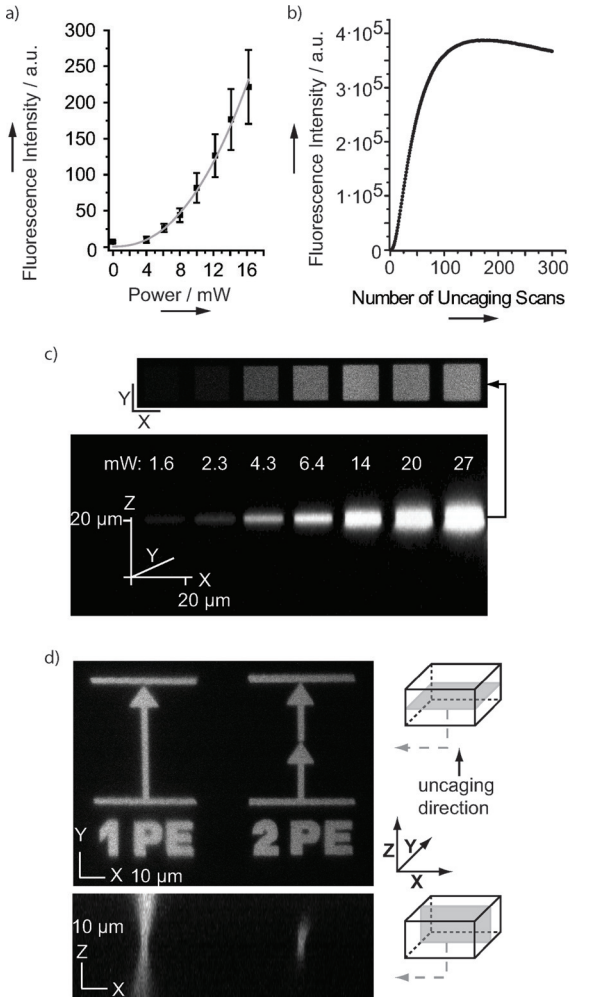

Figure 3. Uncaging properties in a hydrogel-based assay. a) Dependence of the emerging fluorescence on the uncaging power (fitting to the equation $y = a + b\,x^c$ yields $c = 2.28 \pm 0.13$). b) Fluorescence increase over the indicated number of scans in the same area (uncaging pixel dwell time: 2.55 µs). c) Overview of the spatial resolution upon uncaging of square region with increasing power. d) Two perpendicular optical slices of a hydrogel into which simplified energy-level diagrams were drawn. The left diagram was created by one-photon uncaging at 390 nm, whereas the right diagram was written by two-photon uncaging at 780 nm.

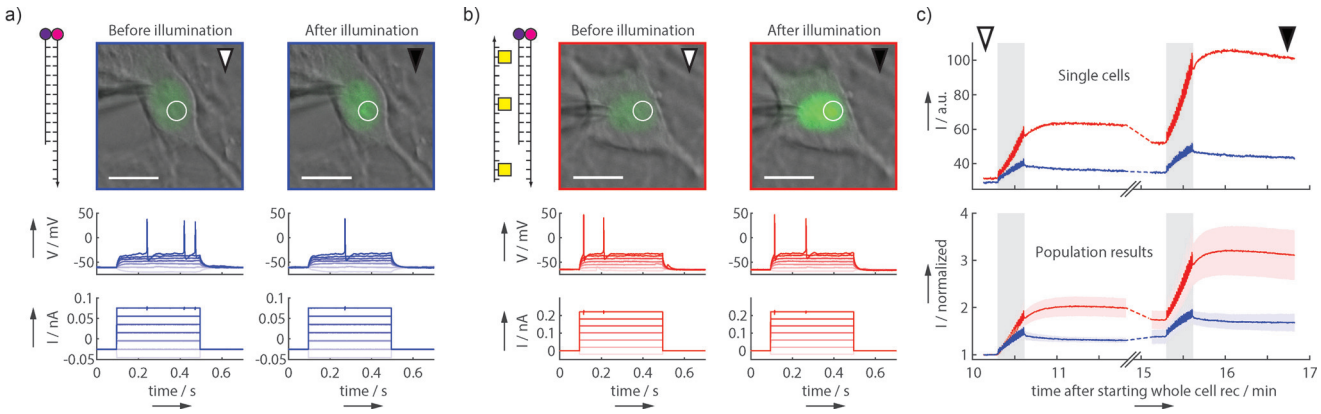

Figure 4. Hippocampal neurons (primary culture), filled with a) the duplex probe (see Figure 2) alone and b) the duplex probe together with **DNA1** through a patch pipette (visible to the left of the cells), were holographically illuminated at 780 nm for two-photon excitation (white circle indicates the location of the illumination spot, scale bar: 10 μm). Electrophysiological properties of the cells were quantified by using current injections (current-clamp traces below cell images in (a) and (b)) before the start and after the end of the illumination procedure (left and right graphs, respectively). c) Fluorescence signals (averaged over the nuclei of the cells) in response to illumination. The gray regions indicate periods of pulsed illumination (10 mW, 20 pulses, 2 ms pulse duration at 1 Hz); blue traces represent cells without, red traces cells with **DNA1**. The results for the individual cells in (a) and (b) are shown (top) as well as population results (bottom, $n = 6$ cells for each set of conditions; solid lines show mean values after normalization, and color-shaded areas indicate mean ± s.e.m.). Graphs in (a) and (b) correspond to the time points indicated by the open and filled arrowheads ("before" and "after illumination", respectively). s.e.m. = standard error of the mean.

points in Figure 3a, a line was scanned four times, and the emerging epifluorescence was quantified. This set of experiments was performed in triplicate. Importantly, Figure 3a shows that the fluorescence generated increases with the square of the power of the incident laser, as predicted by the theory of two-photon excitation.[47] This result demonstrates clearly that the setup was operated in a two-photon regime. The use of a higher power leads to different curve forms and eventually to local melting of the gel as a result of heat effects (data not shown). Figure 3b shows the results obtained when the hydrogel was scanned/uncaged at constant power (4.3 mW, 780 nm) in the form of a square with the indicated number of scans while the emerging fluorescence was quantified by confocal imaging at 561 nm in the focal plane. It can be seen that there is a linear regime, after which the local areas are depleted from the caged precursor, and bleaching of the fluorophore starts to occur. Finally, Figure 3c gives a three-dimensional impression of two-photon uncaging. In this set of experiments, a square region was scanned 20 times. With increasing power, the z-resolution remained very good (for example, 4 μm at 6.4 mW) and then became gradually worse, and bleaching in the focal plane started to occur beyond 14 mW (as can be seen slightly in the optical slice in Figure 3c, top).

Figure 3d shows a direct comparison of one- and two-photon uncaging in the hydrogel. For this purpose, a simplified energy-level diagram was scanned into the hydrogel. Two-photon uncaging was performed at 780 nm (60 scans, 5.3 mW), whereas for one-photon uncaging, this laser beam was frequency-doubled (4 scans, 0.8 mW). Two optical slices of the fluorescence (557–612 nm) are shown. The top of Figure 3d shows a horizontal slice of the figures written, and the bottom picture shows a vertical slice. The latter clearly shows the power of two-photon uncaging: In the case of one-photon uncaging, no resolution in the z-direction was obtained, whereas with two-photon excitation the resolution in z-direction is evident. (For more examples and videos, see the Supporting Information.)

To demonstrate that the uncaging conditions used are compatible with living cells, we introduced the duplex probe with and without **DNA1** into hippocampal neurons and performed localized irradiation (Figure 4). Current injections before and after two-photon illumination show that the physiological function remained unharmed, as the spike threshold and the resting membrane potential remained the same (compare the different shades of the traces corresponding to different current increases in the middle and bottom parts of Figures 4a,b). Evaluation of the fluorescence over time (Figure 4c) shows a degree of dose-dependent local melting of the duplex probe (blue traces) during illumination (gray bars). After illumination, the two strands slowly reassociate over time. In the presence of **DNA1** (red traces), this reassociation is followed by rehybridization, which leads to a substantial increase in the fluorescence signal.

To push complex uncaging further to the limits and test the possibilities of two-photon orthogonal uncaging, we then used **DNA1** and **DNA2** together in the same hydrogel and applied different irradiation parameters and schemes (Figure 5). By setting the uncaging wavelength to 840 nm and restricting the power (1.3 mW), it was possible to only uncage **DNA1**, while leaving the cages on **DNA2** intact. Conversely, by irradiating at 980 nm (8 mW), we were able to selectively uncage **DNA2**, while leaving the cages on **DNA1** intact. Either the sequential application of these two sets of irradiation conditions or irradiation at 840 nm with higher power (13 mW) led to the uncaging of both **DNA1** and **DNA2** (see Figure S3 for the absorption spectra of both caging groups). We used this behavior to write complex two-color patterns into the hydrogel. Uncaging schemes for laser

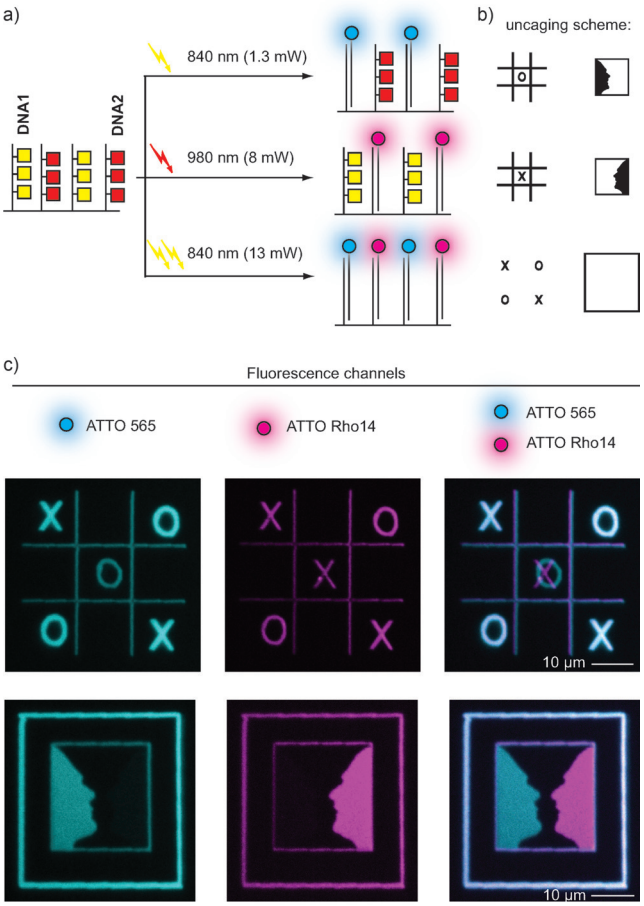

Figure 5. Wavelength-selective (orthogonal) uncaging: **DNA 1** and **DNA 2** were immobilized in the same gel, which also contained the two corresponding fluorescent probes. a) Overview of the selective uncaging strategy. b) Respective schemes used for irradiating the hydrogel. c) Confocal images of the irradiated area after applying the above uncaging schemes. The ATTO 565 channel is shown in cyan, the ATTO Rho14 channel in magenta. The pictures of the right-hand side are an overlay of the images to the left.

scanning to generate pictures of a tic-tac-toe game and the Rubin vase are shown in Figure 5b, and the results in Figure 5c.

The images in Figure 5c show the fluorescence in the ATTO 565 channel (uncaging of **DNA 1**) and the ATTO Rho14 channel (uncaging of **DNA 2**) and an overlay of both images. Features for the controlled uncaging of all possible combinations are clearly visible. For example, uncaging of the area of the left face with low-power irradiation at 840 nm only resulted in a signal in the cyan-colored channel but not in the magenta-colored channel, and conversely for the right face, which was obtained by uncaging **DNA 2** at 980 nm. Uncaging of the outer square at 840 nm with higher power (13 mW) gave a signal in both channels, as did sequential uncaging at 840 nm (1.3 mW) and 980 nm (inner square).

In summary, we have successfully introduced the two-photon uncaging of DNA. A fluorescence-based strand-displacement assay in a hydrogel and in neurons served as the readout and enabled us to establish parameters for well-defined three-dimensional uncaging. The irradiation powers used were below or within the range of powers that are routinely used for two-photon imaging of live tissues. We and others have previously shown that the photocontrol of hybridization by the use of nucleobase-caged DNA and RNA is a very general approach to confer light regulation to a large array of nucleic-acid-based techniques,[2–6,8,48] as hybridization or the interaction of proteins with hybridized sequences are key to the regulation of biological function and nanoarchitectures. Now even three-dimensional resolution will be possible. By using a second caging group with different spectral properties, we have also shown that it is possible to perform the selective uncaging of one group over the other. All of these results pave the way to ever more complex scenarios of light control. We envision applications in brain tissue in vivo through cranial windows,[49] as well as in the developmental biology of model organisms, whereby single cells of an embryo can be addressed at a given developmental stage or through targeted drug release even in the presence of blood.

Acknowledgements

This research was supported by the Deutsche Forschungsgemeinschaft (GRK 1986—CLiC), the Fonds der Chemischen Industrie (fellowship to M.A.H.F.), and the ANR (Contract No. ANR-13-JSJV-0009-01). The company Rapp OptoElectronic provided major technical support. We gratefully acknowledge help by the Heilemann group and by Erin Schuman (Frankfurt). We also thank Ina Bartnik, Nicole Fuerst, and Anja Stab for the preparation of cultured hippocampal neurons.

Keywords: DNA · hydrogels · photochemistry · two-photon uncaging · wavelength selectivity

How to cite: *Angew. Chem. Int. Ed.* **2016**, *55*, 8948–8952
Angew. Chem. **2016**, *128*, 9094–9098

[1] W. Szymański, J. M. Beierle, H. A. V. Kistemaker, W. A. Velema, B. L. Feringa, *Chem. Rev.* **2013**, *113*, 6114–6178.
[2] Z. Feng, W. Zhang, J. Xu, C. Gauron, B. Ducos, S. Vriz, M. Volovitch, L. Jullien, S. Weiss, D. Bensimon, *Rep. Prog. Phys.* **2013**, *76*, 072601.
[3] A. Gautier, C. Gauron, M. Volovitch, D. Bensimon, L. Jullien, S. Vriz, *Nat. Chem. Biol.* **2014**, *10*, 533–541.
[4] C. Brieke, F. Rohrbach, A. Gottschalk, G. Mayer, A. Heckel, *Angew. Chem. Int. Ed.* **2012**, *51*, 8446–8476; *Angew. Chem.* **2012**, *124*, 8572–8604.
[5] A. Specht, F. Bolze, Z. Omran, J.-F. Nicoud, M. Goeldner, *HFSP J.* **2009**, *3*, 255–264.
[6] G. C. R. Ellis-Davies, *Nat. Methods* **2007**, *4*, 619–628.
[7] P. Klán, T. Šolomek, C. G. Bochet, A. Blanc, R. Givens, M. Rubina, V. Popik, A. Kostikov, J. Wirz, *Chem. Rev.* **2013**, *113*, 119–191.
[8] M. J. Hansen, W. A. Velema, M. M. Lerch, W. Szymanski, B. L. Feringa, *Chem. Soc. Rev.* **2015**, *44*, 3358–3377.
[9] F. Buhr, J. Kohl-Landgraf, S. tom Dieck, C. Hanus, D. Chatterjee, A. Hegelein, E. M. Schuman, J. Wachtveitl, H. Schwalbe, *Angew. Chem. Int. Ed.* **2015**, *54*, 3717–3721; *Angew. Chem.* **2015**, *127*, 3788–3792.

[10] D. D. McKinnon, T. E. Brown, K. A. Kyburz, E. Kiyotake, K. S. Anseth, *Biomacromolecules* **2014**, *15*, 2808 – 2816.
[11] V. San Miguel, M. Álvarez, O. Filevich, R. Etchenique, A. del Campo, *Langmuir* **2012**, *28*, 1217 – 1221.
[12] J. H. Wosnick, M. S. Shoichet, *Chem. Mater.* **2008**, *20*, 55 – 60.
[13] T. L. Schmidt, M. B. Koeppel, J. Thevarpadam, D. P. N. Gonçalves, A. Heckel, *Small* **2011**, *7*, 2163 – 2167.
[14] W. Ji, N. Li, D. Chen, X. Qi, W. Sha, Y. Jiao, Q. Xu, J. Lu, *J. Mater. Chem. B* **2013**, *1*, 5942 – 5949.
[15] S. Samanta, A. Babalhavaeji, M. Dong, G. A. Woolley, *Angew. Chem. Int. Ed.* **2013**, *52*, 14127 – 14130; *Angew. Chem.* **2013**, *125*, 14377 – 14380.
[16] R. Weissleder, *Nat. Biotechnol.* **2001**, *19*, 316 – 317.
[17] G. Bort, T. Gallavardin, D. Ogden, P. I. Dalko, *Angew. Chem. Int. Ed.* **2013**, *52*, 4526 – 4537; *Angew. Chem.* **2013**, *125*, 4622 – 4634.
[18] M. Goeldner, R. Givens, *Dynamic Studies in Biology*: *Phototriggers*, *Photoswitches and Caged Biomolecules*, Wiley-VCH, Weinheim, **2005**.
[19] T. Furuta, S. S.-H. Wang, J. L. Dantzker, T. M. Dore, W. J. Bybee, E. M. Callaway, W. Denk, R. Y. Tsien, *Proc. Natl. Acad. Sci. USA* **1999**, *96*, 1193 – 1200.
[20] J. P. Olson, H.-B. Kwon, K. T. Takasaki, C. Q. Chiu, M. J. Higley, B. L. Sabatini, G. C. R. Ellis-Davies, *J. Am. Chem. Soc.* **2013**, *135*, 5954 – 5957.
[21] J. M. Amatrudo, J. P. Olson, G. Lur, C. Q. Chiu, M. J. Higley, G. C. R. Ellis-Davies, *ACS Chem. Neurosci.* **2014**, *5*, 64 – 70.
[22] C. Bao, G. Fan, Q. Lin, B. Li, S. Cheng, Q. Huang, L. Zhu, *Org. Lett.* **2012**, *14*, 572 – 575.
[23] O. D. Fedoryak, T. M. Dore, *Org. Lett.* **2002**, *4*, 3419 – 3422.
[24] M. Petit, C. Tran, T. Roger, T. Gallavardin, H. Dhimane, F. Palma-Cerda, M. Blanchard-Desce, F. C. Acher, D. Ogden, P. I. Dalko, *Org. Lett.* **2012**, *14*, 6366 – 6369.
[25] G. Papageorgiou, M. Lukeman, P. Wan, J. E. T. Corrie, *Photochem. Photobiol. Sci.* **2004**, *3*, 366 – 373.
[26] N. Gagey, P. Neveu, L. Jullien, *Angew. Chem. Int. Ed.* **2007**, *46*, 2467 – 2469; *Angew. Chem.* **2007**, *119*, 2519 – 2521.
[27] K. Korzycka, P. M. Bennett, E. J. Cueto-Diaz, G. Wicks, M. Drobijev, M. Blanchard-Desce, A. Rebane, H. L. Anderson, *Chem. Sci.* **2015**, *6*, 2419 – 2426.
[28] A. Momotake, N. Lindegger, E. Niggli, R. J. Barsotti, G. C. R. Ellis-Davies, *Nat. Methods* **2006**, *3*, 35 – 40.
[29] I. Aujard, C. Benbrahim, M. Gouget, O. Ruel, J.-B. Baudin, P. Neveu, L. Jullien, *Chem. Eur. J.* **2006**, *12*, 6865 – 6879.
[30] A. Specht, F. Bolze, L. Donato, C. Herbivo, S. Charon, D. Warther, S. Gug, J.-F. Nicoud, M. Goeldner, *Photochem. Photobiol. Sci.* **2012**, *11*, 578 – 586.
[31] N. Komori, S. Jakkampudi, R. Motoishi, M. Abe, K. Kamada, K. Furukawa, C. Katan, W. Sawada, N. Takahashi, H. Kasai, B. Xue, T. Kobayashi, *Chem. Commun* **2016**, *52*, 331 – 334.
[32] L. Donato, A. Mourot, C. M. Davenport, C. Herbivo, D. Warther, J. Léonard, F. Bolze, J.-F. Nicoud, R. H. Kramer, M. Goeldner, A. Specht, *Angew. Chem. Int. Ed.* **2012**, *51*, 1840 – 1843; *Angew. Chem.* **2012**, *124*, 1876 – 1879.
[33] L. García-Fernández, C. Herbivo, V. S. M. Arranz, D. Warther, L. Donato, A. Specht, A. del Campo, *Adv. Mater.* **2014**, *26*, 5012 – 5017.
[34] J. Luo, R. Uprety, Y. Naro, C. Chou, D. P. Nguyen, J. W. Chin, A. Deiters, *J. Am. Chem. Soc.* **2014**, *136*, 15551 – 15558.
[35] V. Gatterdam, R. Ramadass, T. Stoess, M. A. H. Fichte, J. Wachtveitl, A. Heckel, R. Tampé, *Angew. Chem. Int. Ed.* **2014**, *53*, 5680 – 5684; *Angew. Chem.* **2014**, *126*, 5787 – 5791.
[36] K. M. Schelkle, T. Griesbaum, D. Ollech, S. Becht, T. Buckup, M. Hamburger, R. Wombacher, *Angew. Chem. Int. Ed.* **2015**, *54*, 2825 – 2829; *Angew. Chem.* **2015**, *127*, 2867 – 2871.
[37] M. Goard, G. Aakalu, O. D. Fedoryak, C. Quinonez, J. St. Julien, S. J. Poteet, E. M. Schuman, T. M. Dore, *Chem. Biol.* **2005**, *12*, 685 – 693.
[38] H. Lusic, R. Uprety, A. Deiters, *Org. Lett.* **2010**, *12*, 916 – 919.
[39] T. Furuta, T. Watanabe, S. Tanabe, J. Sakyo, C. Matsuba, *Org. Lett.* **2007**, *9*, 4717 – 4720.
[40] M. K. G. Jayakumar, N. M. Idris, Y. Zhang, *Proc. Natl. Acad. Sci. USA* **2012**, *109*, 8483 – 8488.
[41] Y. Yang, F. Liu, X. Liu, B. Xing, *Nanoscale* **2013**, *5*, 231 – 238.
[42] X. Ouyang, I. A. Shestopalov, S. Sinha, G. Zheng, C. L. W. Pitt, W.-H. Li, A. J. Olson, J. K. Chen, *J. Am. Chem. Soc.* **2009**, *131*, 13255 – 13269.
[43] C. G. Bochet, *Pure Appl. Chem.* **2006**, *78*, 241 – 247.
[44] S. Kantevari, M. Matsuzaki, Y. Kanemoto, H. Kasai, G. C. R. Ellis-Davies, *Nat. Methods* **2010**, *7*, 123 – 125.
[45] A. Rodrigues-Correia, X. M. M. Weyel, A. Heckel, *Org. Lett.* **2013**, *15*, 5500 – 5503.
[46] Q. Li, G. Luan, Q. Guo, J. Liang, *Nucleic Acids Res.* **2002**, *30*, e5.
[47] W. Kaiser, C. G. B. Garrett, *Phys. Rev. Lett.* **1961**, *7*, 229 – 231.
[48] F. Schäfer, J. Wagner, A. Knau, S. Dimmeler, A. Heckel, *Angew. Chem. Int. Ed.* **2013**, *52*, 13558 – 13561; *Angew. Chem.* **2013**, *125*, 13801 – 13805.
[49] S. E. Crowe, G. C. R. Ellis-Davies, *J. Comp. Neurol.* **2014**, *522*, 1708 – 1727.

Received: April 7, 2016
Published online: June 13, 2016

